Article

Tooth Movement Patterns Based on Traction Methods for Mandibular Canine Retraction Using Skeletal Anchorage: A Finite Element Analysis

Dong-Hwan Lee; Sung-Kwon Choi; Kyung-Hwa Kang
University of Wonkwang,
Department of Orthodontics, College of Dentistry

Objectives

This study compared the tooth movement patterns of a power arm and a lever jig during mandibular canine retraction into a premolar extraction space using skeletal anchorage.

Introduction

Effective posterior retraction of the canine is critical in premolar extraction cases. However, its apically positioned center of resistance often leads to undesired distal tipping and vertical bowing during retraction. Conventional methods, such as power arms and rigid archwires, partially mitigate these effects but cannot fully prevent them. The lever jig, based on the first-class lever principle, offers controlled moment-to-force ratios, potentially enhancing the predictability of tooth movement. Finite Element Analysis(FEA) was employed to simulate and compare the biomechanical responses of different retraction strategies, including the lever jig and conventional power arm setups.

Materials & Methods

① *Fabrication of the Lever jig*

The lever jig(**Fig. 1**) is made from 0.016 × 0.022-inch stainless steel wire, providing sufficient rigidity to resist deformation under orthodontic forces. It is positioned between the main archwire and the tooth, with a minimal horizontal arm and a vertical arm adjustable between 6–10 mm to control the moment-to-force (M/F) ratio. A 100° angle between the arms ensures fulcrum stability during force applications.

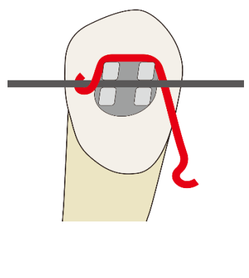

Fig 1. Configuration of a lever jig

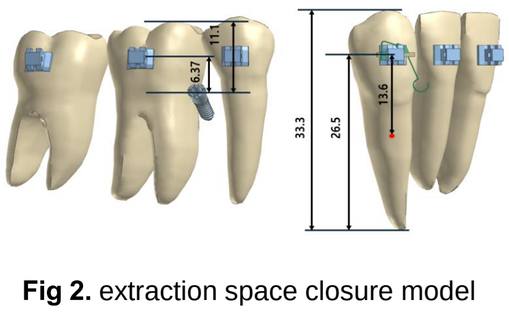

Fig 2. extraction space closure model

② *Experimental Design*

To analyze sliding mechanics during extraction space closure, two models were compared: one using a power arm and the other a lever jig. In both, force was applied from an orthodontic mini-implant (1.6 mm × 6 mm) placed between the mandibular second premolar and first molar(**Fig. 2**), positioned to direct force above the canine's center of resistance(**Fig. 3**). Vertical positions of key reference points—including the mini-implant, force application point, and canine's center of resistance—were measured relative to the main archwire.

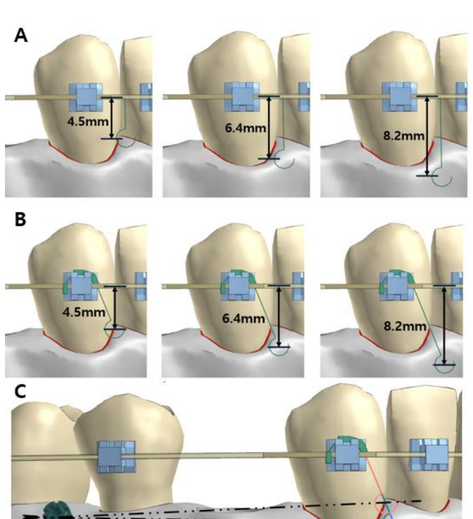

Figure 3. Vertical positioning of the power arm and lever jig with corresponding force vectors. (A) Configuration of the power arm with vertical lengths of 4.5 mm, 6.4 mm, and 8.2 mm. (B) Configuration of the lever jig, with vertical distance of 4.5 mm, 6.4 mm, and 8.2 mm, corresponding to vertical arm lengths of 6 mm, 8 mm, and 10 mm, respectively. (C) Schematic representation of the force vectors generated by the power arm and lever jig.

③ *Finite Element Analysis (FEA) Modeling*

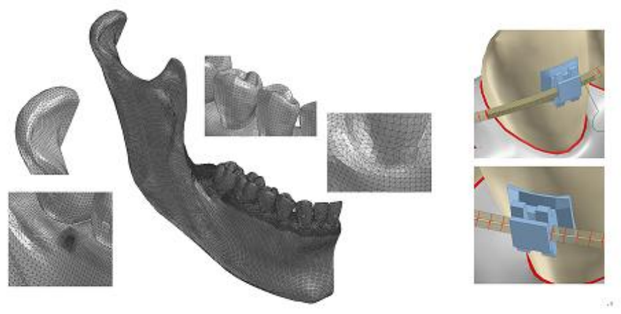

Fig. 4 A tetrahedral mesh was generated in Visual Crash for PAM. To simplify the analysis, symmetry of the dental arch was assumed, and only the lower right mandible—including tooth, bracket, archwire, and alveolar bone—was modeled. The alveolar bone was divided into cortical and cancellous components to reflect its biomechanical properties

④ *Material Properties*

Component	Young's Modulus	Poisson's Ratio
PDL	18Mpa	0.45
Cortical bone	14Gpa	0.30
Trabecular bone	1.4Gpa	0.30
Stainless steel wire	200Gpa	0.30

Table1. Mechanical properties of the mechanical variables.

⑤ *Loading and Boundary Conditions*

- a nonlinear static implicit method.
- Retraction force was gradually increased to 5 N under quasi-static conditions.
- Simulations were conducted with VPS (version 2023.0), and results were visualized using Visual Viewer (version 2024.0; ESI Group, Paris, France).

⑥ *Coordinate System*

- Positive *X*-axis: Mesial direction
- Positive *Y*-axis: Lingual direction
- Positive *Z*-axis: Coronal direction

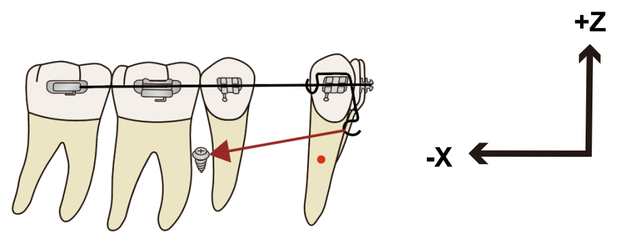

⑦ *Dynamic Simulation of Initial Tooth Movement Process*

- The load transmitted to the bracket
- The displacement of the mandibular canine
- The distribution of tensile and compressive stress in the PDL

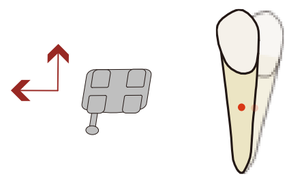

Results

① *Load Transmission to the Bracket*

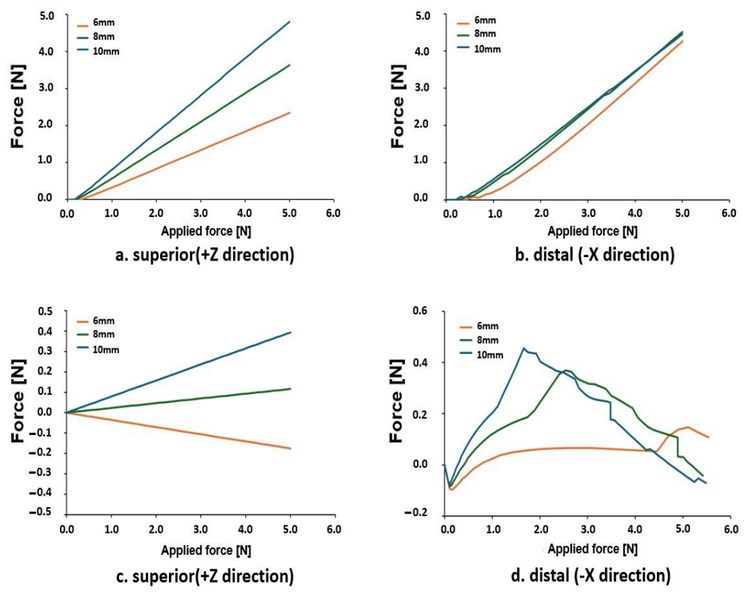

- In the power arm model, longer arm lengths increased force transmission in both directions, with reduced loss in the superior direction; however, distal forces showed little difference between 8 mm
- and 10 mm arms.
- the lever jig model showed a dynamic force pattern: initial upward force shifted downward and backward as the jig contacted the bracket, resulting in more stable and consistent force transmission.

Fig. 5 Forces transmitted to the bracket in the superior (+Z) and distal (−X) directions were analyzed for both the power arm(a,b) and lever jig(c,d) models

② *Initial Displacement Pattern of the Canine*

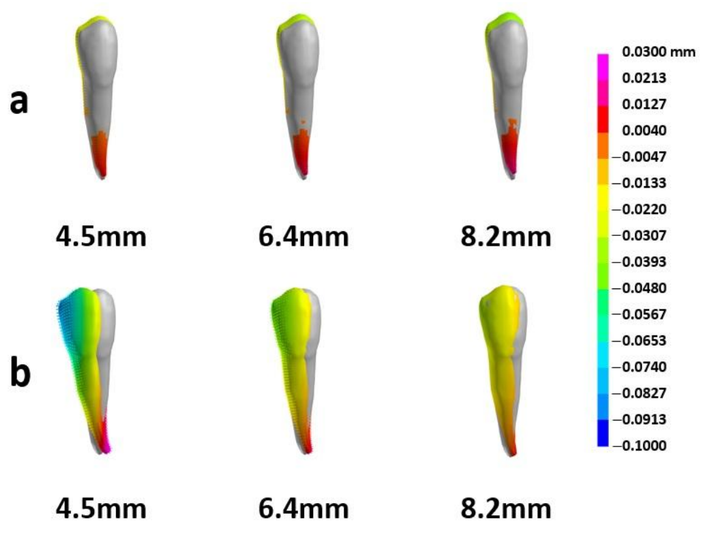

- In the power arm model, longer arms increased crown extrusion and distal tipping, with a greater displacement gap between the crown and root apex.
- the lever jig model showed reduced distal tipping and a smaller crown–root displacement difference as jig length increased.

Fig. 6 Contour plot of initial canine displacement when using a power arm(a) and a lever jig(b)

③ *Tensile & Compressive Stress Distribution in the PDL*

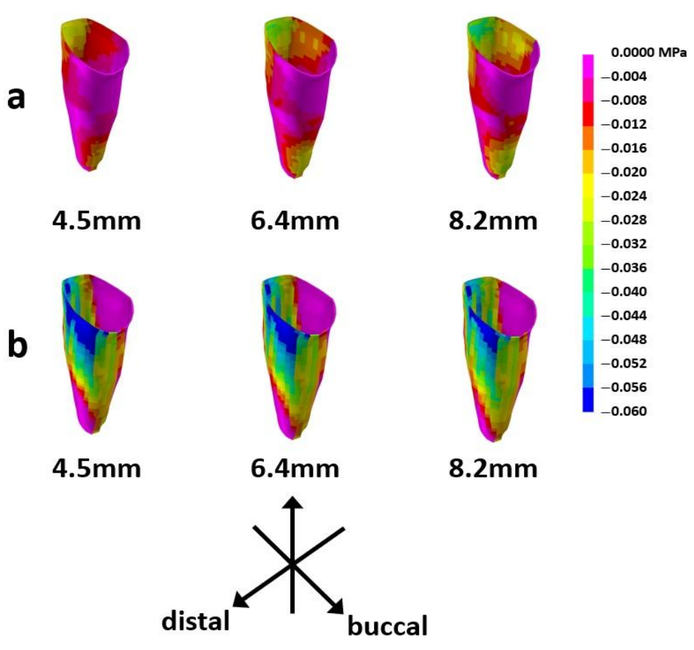

Figure 7. Tensile stress in the PDL when using a power arm (**a**) and a lever jig **(b)**

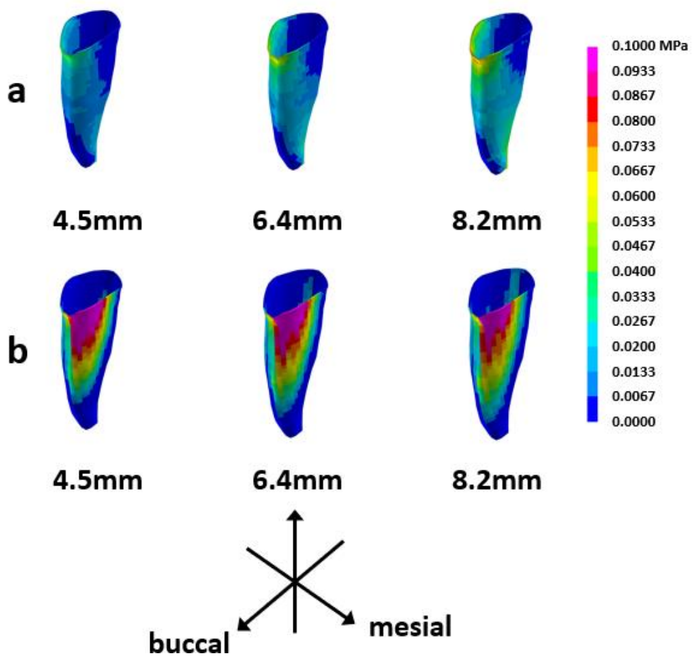

Figure 8. Compressive stress in the PDL when using a power arm (**a**) and a lever jig **(b)**

Conclusion

Based on this study, the lever jig may offer several advantages over the power arm in clinical orthodontics.

1. **Efficient force redirection and minimization of unnecessary vertical displacement**
2. **Minimization of tipping and maintenance of an optimal moment-to-force ratio for controlled translation**
3. **Balanced stress distribution in the PDL with reduced localized stress concentration**
4. **Reduced reliance on additional mechanics through natural control of tipping and extrusion**